Binuclear Iron System Ferromagnetic in Three Oxidation States: Synthesis, Structures, and Electronic Aspects of Molecules with a $Fe_2(OR)_2$ Bridge Unit Containing Fe(III,III), Fe(III,II), and Fe(II,II)

Barry S. Snyder, George S. Patterson,[1] Andrew J. Abrahamson, and R. H. Holm*

Contribution from the Department of Chemistry, Harvard University, Cambridge, Massachusetts 02138. *Received January 3, 1989*

Abstract: The Fe(III) complex of the pentadentate ligand 2-bis(salicylideneamino)methylphenolate(3-) (**4**, salmp), first prepared in 1935, has been investigated in the context of the increasing interest in oxygen-bridged binuclear Fe units in biology and models thereof and in the phenomenon of ferromagnetism. The established bridge units of this type are summarized. The complex $Fe_2(salmp)_2 \cdot 2DMF$ (**6**) crystallizes in monoclinic space group $P2_1/c$ with a = 9.907 (5) Å, b = 10.584 (6) Å, c = 20.709 (6) Å, β = 93.28 (3)°, and Z = 2. The molecule has imposed centrosymmetry and contains two trans FeN_2O_4 distorted octahedral coordination units bridged by two phenolate oxygen atoms. This ligand conformation leads to C_{2h} symmetry and is essentially constant in lower oxidation states. Complex **6** undergoes two reversible electron-transfer reactions at $E_{1/2}$ = -0.46 and -1.00 V vs SCE, affording $[Fe_2(salmp)_2]^-$ (**8**) and $[Fe_2(salmp)_2]^{2-}$ (7), respectively. Complex 7, prepared by the reaction of **4** with $FeCl_2$ or by chemical reduction of **6**, was obtained as $(Et_4N)_2[7] \cdot 4MeCN$ in space group $P2_1/c$ with a = 18.248 (5) Å, b = 15.454 (6) Å, c = 23.321 (6) Å, β = 96.64 (3)°, and Z = 4. Mixed valence complex **8**, prepared by the reduction of **6** with HS^- or by comproportionation of **6** and 7 ($K_{com} = 1.4 \times 10^9$) and obtained as $(Et_4N)[8] \cdot 2DMF$, crystallizes in triclinic space group $P\bar{1}$ with a = 12.669 (3) Å, b = 12.992 (2) Å, c = 16.928 (4) Å, α = 99.27 (2)°, β = 101.54 (2)°, γ = 95.91 (2)°, and Z = 2. The dimensions of **7** generally reflect the difference in radii of high-spin Fe(II) and Fe(III) (0.13 Å), while those of **8**, which has imposed centrosymmetry, are rough averages of **6** and 7. The set of three complexes is unique in several significant respects: **4** forms centrosymmetric bis complexes containing octahedral sites without requiring exogenous ligands; the $Fe^{III}_2(OPh)_2$ bridge has the smallest Fe-O-Fe angle (97°) and Fe-Fe separation (3.06 Å) yet found for the generalized $Fe_2(OR)_2$ bridge; three oxidation levels are related by reversible redox reactions and have been isolated and their structures determined; the complexes **6**, 7, and **8** are *ferromagnetic* with ground states S = 5, $^9/_2$, and 4, respectively. The magnetic properties were established from magnetic susceptibilities determined at 6-300 K. Ferromagnetic exchange energies are small; J = 1.2 (**6**, 7) and 8.6 (**8**) cm^{-1}. All other complexes with the $Fe_2(OR)_2$ bridge are antiferromagnetic. Further, all binuclear Fe(III) complexes are antiferromagnetic except for two which are triply bridged by octahedral face-sharing. The effects of distortions of bridge angle, axial N-Fe-N bond angles, out-of-plane distortions of terminal oxygen atoms, and Fe-O bond distances in the bridge on the energies of d-block molecular orbitals were examined. These results afford the qualitative conclusion that the distorted coordination stereochemistry observed in **6** is such as to promote a ferromagnetic ground state vs the case of an idealized binuclear complex with 90° bond angles and D_{2h} symmetry.

The chemistry of binuclear oxygen-bridged iron complexes has experienced a resurgence of interest with the discovery of bridged units of this general type in a number of nonheme proteins and enzymes.[2] With the exception of the hydrolysis products of Fe(III),[3,4] whose exact nature remains controversial, the first binuclear oxo-bridged complex to have been prepared and properly formulated was $[Fe(salen)_2]O$,[5] obtained by Pfeiffer et al.[6] in 1933. This is the prototype of complexes with the unsupported μ-oxo bridge **1a**[7] depicted in Figure 1. These species exhibit strong antiferromagnetic coupling between the two high-spin Fe(III) atoms that is dependent on the Fe-O-Fe bridge angle.[8] All other known bridge structures in *binuclear* molecular Fe complexes are set out in Figure 1.

Bridge **1b** has been prepared with R = *p*-phenylene and related groups.[9] The single example of the μ-oxo/μ-carboxylato bridge **2a** has R = Ph.[10] Numerous bridges of type **2b** have been characterized and include cases with R = H,[11] alkyl, and aryl and mixtures thereof.[12,13] The μ-oxo/bis(μ-carboxylato) unit **3a**[2,14]

(1) Department of Chemistry, Suffolk University, Boston, MA 02114.
(2) Lippard, S. J. *Angew. Chem., Int. Ed. Engl.* **1988**, *27*, 344.
(3) (a) Knudsen, J. M.; Larsen, E.; Moreira, J. E.; Nielsen, O. F. *Acta Chem. Scand.* **1975**, *A29*, 833. (b) Morrison, T. I.; Reis, A. H., Jr.; Knapp, G. S.; Fradin, F. Y.; Chen, H.; Klippert, T. E. *J. Am. Chem. Soc.* **1978**, *100*, 3262. (c) Khoe, G. H.; Brown, P. L.; Sylva, R. N.; Robins, R. G. *J. Chem. Soc., Dalton Trans.* **1986**, 1901, and references therein.
(4) Flynn, C. M., Jr. *Chem. Rev.* **1984**, *84*, 31.
(5) Abbreviations: acac, acetylacetonate(1-); bpmp, 2,6-bis[bis(2-pyridylmethyl)aminomethyl]-4-methylphenolate(1-) (**11**); bzim, 2,6-bis[bis-(2-benzimidazolylmethyl)aminomethyl]-4-methylphenolate(1-); $HBpz_3$, tris(pyrazolyl)borate(1-); hxta, *N,N'*-(2-hydroxy-5-methyl-1,3-xylylene)bis-(*N*-carboxymethyl)glycinate(5-) (**10**); Im, imidazole; Me_3tacn, 1,4,7-trimethyl-1,4,7-triazacyclononane; salen, 1,2-bis(salicylideneamino)ethane(2-); P, porphyrinate(2-); salmp, bis(salicylideneamino)-2-methylphenolate(3-) (**4**); saltrien, 1,3-bis(salicylideneaminoethyl)-2-(2-hydroxyphenyl)-1,3-diazacyclopentane(3-) (**9**).
(6) Pfeiffer, P.; Breith, E.; Lübbe, E.; Tsumaki, T. *Justus Liebigs Ann. Chem.* **1933**, *503*, 84.
(7) Murray, K. S. *Coord. Chem. Rev.* **1974**, *12*, 1.
(8) Mukherjee, R. N.; Stack, T. D. P.; Holm, R. H. *J. Am. Chem. Soc.* **1988**, *110*, 1850, and references therein.
(9) (a) Floriani, C.; Fachinetti, G.; Calderazzo, F. *J. Chem. Soc., Dalton Trans.* **1973**, 765. (b) Kessel, S. L.; Hendrickson, D. N. *Inorg. Chem.* **1978**, *17*, 2630. (c) Heistand, R. H., II; Roe, A. L.; Que, L., Jr. *Inorg. Chem.* **1982**, *21*, 676.
(10) Yan, S.; Que, L., Jr.; Taylor, L. F.; Anderson, O. P. *J. Am. Chem. Soc.* **1988**, *110*, 5222.
(11) (a) Thich, J. A.; Ou, C. C.; Powers, D.; Vasiliou, B.; Mastropaolo, D.; Potenza, J. A.; Schugar, H. J. *J. Am. Chem. Soc.* **1976**, *98*, 1425. (b) Ou, C. C.; Lalancette, R. A.; Potenza, J. A.; Schugar, H. J. *J. Am. Chem. Soc.* **1978**, *100*, 2053. (c) Borer, L.; Thalken, L.; Ceccarelli, C.; Glick, M.; Zhang, J. H.; Reiff, W. M. *Inorg. Chem.* **1983**, *22*, 1719.
(12) (a) Gerloch, M.; Mabbs, F. E. *J. Chem. Soc. A* **1967**, 1900. (b) Bertrand, J. A.; Breece, J. L.; Eller, P. G. *Inorg. Chem.* **1974**, *13*, 125. (c) Bertrand, J. A.; Eller, P. G. *Inorg. Chem.* **1974**, *13*, 927. (d) Long, G. J.; Wrobleski, J. T.; Thundathil, R. V.; Sparlin, D. M.; Schlemper, E. O. *J. Am. Chem. Soc.* **1980**, *102*, 6040. (e) Barclay, S. J.; Riley, P. E.; Raymond, K. N. *J. Am. Chem. Soc.* **1982**, *104*, 6802. (f) Ainscough, E. W.; Brodie, A. M.; McLachlan, S. J.; Brown, K. L. *J. Chem. Soc., Dalton Trans.* **1983**, 1385. (g) Barclay, S. J.; Riley, P. E.; Raymond, K. N. *Inorg. Chem.* **1984**, *23*, 2005. (h) Murch, B. P.; Boyle, P. D.; Que, L., Jr. *J. Am. Chem. Soc.* **1985**, *107*, 6728. (i) Murch, B. P.; Bradley, F. C.; Boyle, P. D.; Papaefthymiou, V.; Que, L., Jr. *J. Am. Chem. Soc.* **1987**, *109*, 7993. (j) Spartalian, K.; Bonadies, J. A.; Carrano, C. J. *Inorg. Chim. Acta* **1988**, *152*, 135.
(13) (a) Lambert, S. L.; Hendrickson, D. N. *Inorg. Chem.* **1979**, *18*, 2683. (b) Spiro, C. L.; Lambert, S. L.; Smith, T. J.; Duesler, E. N.; Gagne, R. R.; Hendrickson, D. N. *Inorg. Chem.* **1981**, *20*, 1229. (c) Chiari, B.; Piovesana, O.; Tarantelli, T.; Zanazzi, P. F. *Inorg. Chem.* **1984**, *23*, 3398.

0002-7863/89/1511-5214$01.50/0

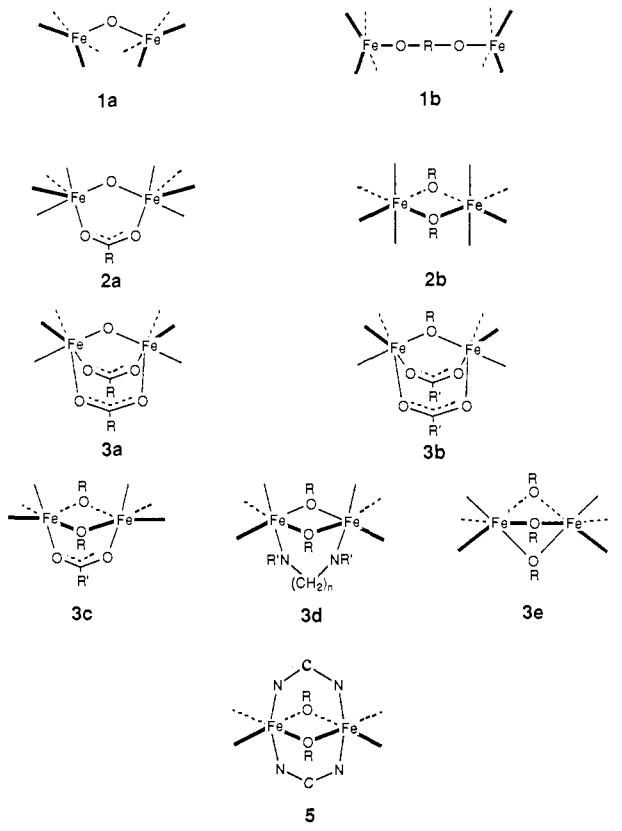

Figure 1. Previously characterized bridge units **1–3** in binuclear Fe complexes. The indicated coordination number and stereochemistry apply to most or all complexes with a given unit. Bridge unit **5** is demonstrated in this work.

(R = H, alkyl, aryl) has been studied in considerable detail; species with phosphodiester[15] in place of carboxylate bridges are a subset of this bridge type. The preceding unit can be formally or actually protonated to afford bridge **3b** (R = H[2,16]); other examples have R = aryl.[17-19] Bridge **3c** is known only in a form with R = aryl and R′ = Me.[20] Bridge unit **3d** contains R = Me or combinations of Me, H, and aryl and in addition an extended bridge in the form of a large ring whose amino nitrogen atoms (R′ = alkyl) are bound to the metal.[13c,21] Bridge **3e**, which is composed of two face-shared octahedra, was first encountered in $Fe_2(acac)_4$[22] and subsequently in $[Fe_2(OH)_3(Me_3tacn)_2]^{2+}$.[23]

It has been established that complexes with bridges **3a** and **3b** (R = H) are excellent representations of the bridge portions of the binuclear sites in met and deoxy hemerythrin,[2,24] respectively. It is probable that ribonucleotide reductase includes a highly similar $Fe_2O(RCO_2)_2$ bridge unit.[25] Methane monooxygenase also contains a binuclear site, but in the semireduced form the relatively short Fe–O distance normally associated with a Fe–O–Fe bridge is absent.[26] Current models for purple acid phosphatase feature Fe–O–Fe and Fe–(OH)–Fe bridges in the oxidized and reduced forms,[27] respectively. Deductions of structural elements present in the binuclear sites of these metallobiomolecules could not have proceeded as effectively without access to synthetic complexes containing these elements.

Complexes containing bridge units **1–3** have certain important features in common. All provide high-spin Fe coordination sites, most contain two Fe(III) atoms as prepared, and all are antiferromagnetically coupled except for one case containing triple-bridge **3e**.[23] However, of the three possible oxidation levels, Fe(III,III), Fe(III,II), and Fe(II,II), only a few complexes, with bridges **2b**,[13] and **3b**,[14c,16a,19] have been obtained in the fully reduced condition. These same bridges have been found to support the mixed-valence oxidation level,[14c,18,19] and the structure of one compound containing **3b** (R = aryl) has been described.[19]

In connection with our recent work on five-coordinate Fe(II)–salen systems,[28] we observed that the compound formulated as the Fe(III) complex of the trianion of "hydrosalicylamide" (**4**)

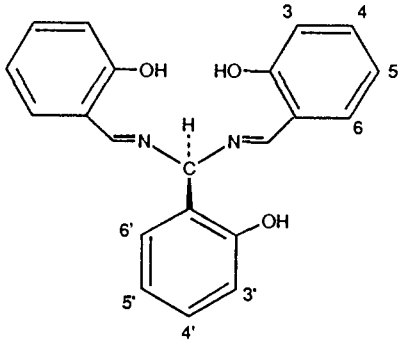

4

was unlikely to conform to the five-coordinate stereochemistry proposed[29] because of excessive strain. Our considerations of this venerable compound, first prepared in 1935[30] and the subject of only one report since (in 1960[29]), indicated that it would more probably have a binuclear structure. In this event, unit **5** (Figure 1), including two intimate (R = Ph) and two extended bridges, would prevail, there being no other feasible bridging mode. Because **5** is an unknown structural entity in the rapidly evolving chemistry of oxygen-bridged binuclear Fe complexes, we have investigated the compound described as "trisalicylaldehydediimine-iron(III)".[29,30] As will be shown, this compound and its reduction products display desirable and unusual properties that clearly demarcate them from complexes with bridges **1–3**. These include reversible electron-transfer reactions between three oxidation levels, stability of each oxidation state sufficient to permit isolation, and ferromagnetic spin coupling in each oxidation level. Additionally, it has proven possible to obtain

(14) (a) Armstrong, W. H.; Spool, A.; Papaefthymiou, G. C.; Frankel, R. B.; Lippard, S. J. *J. Am. Chem. Soc.* **1984**, *106*, 3653. (b) Toftlund, H.; Murray, K. S.; Zwack, P. R.; Taylor, L. F.; Anderson, O. P. *J. Chem. Soc., Chem. Commun.* **1986**, 191. (c) Hartman, J. R.; Rardin, R. L.; Chaudhuri, P.; Pohl, K.; Wieghardt, K.; Nuber, B.; Weiss, J.; Papaefthymiou, G. C.; Frankel, R. B.; Lippard, S. J. *J. Am. Chem. Soc.* **1987**, *109*, 7387. (d) Gomez-Romero, P.; Casan-Pastor, N.; Ben-Hussein, A.; Jameson, G. B. *J. Am. Chem. Soc.* **1988**, *110*, 1988.

(15) Armstrong, W. H.; Lippard, S. J. *J. Am. Chem. Soc.* **1985**, *107*, 3730.

(16) (a) Chaudhuri, P.; Wieghardt, K.; Nuber, B.; Weiss, J. *Angew. Chem., Int. Ed. Engl.* **1985**, *24*, 778. (b) Armstrong, W. H.; Lippard, S. J. *J. Am. Chem. Soc.* **1984**, *106*, 4632.

(17) Murch, B. P.; Bradley, F. C.; Que, L., Jr. *J. Am. Chem. Soc.* **1986**, *108*, 5027.

(18) (a) Suzuki, M.; Uehara, A.; Endo, K. *Inorg. Chim. Acta* **1986**, *123*, L9. (b) Borovik, A. S.; Murch, B. P.; Que, L., Jr.; Papaefthymiou, V.; Münck, E. *J. Am. Chem. Soc.* **1987**, *109*, 7190.

(19) Borovik, A. S.; Que, L., Jr. *J. Am. Chem. Soc.* **1988**, *110*, 2345.

(20) Anderson, B. F.; Webb, J.; Buckingham, D. A.; Robertson, G. B. *J. Inorg. Biochem.* **1982**, *16*, 21.

(21) (a) Bailey, N. A.; McKenzie, E. D.; Worthington, J. M.; McPartlin, M.; Tasker, P. A. *Inorg. Chim. Acta* **1977**, *25*, L137. (b) Chiari, B.; Piovesana, O.; Tarantelli, T.; Zanazzi, P. F. *Inorg. Chem.* **1982**, *21*, 1396, 2444; **1983**, *22*, 2781.

(22) Shibata, S.; Onuma, S.; Iwase, A.; Inoue, H. *Inorg. Chim. Acta* **1977**, *25*, 33.

(23) Drüeke, S.; Chaudhuri, P.; Pohl, K.; Wieghardt, K.; Ding, X. Q.; Bill, E.; Sawaryn, A.; Trautwein, A. X.; Winkler, H.; Gurman, S. J. *J. Chem. Soc., Chem. Commun.* **1989**, 59.

(24) (a) Klotz, I. M.; Kurtz, D. M., Jr. *Acc. Chem. Res.* **1984**, *17*, 16. (b) Wilkins, P. C.; Wilkins, R. G. *Coord. Chem. Rev.* **1987**, *79*, 195.

(25) (a) Reichard, P.; Ehrenberg, A. *Science* **1983**, *221*, 514. (b) Scarrow, R. C.; Maroney, M. J.; Palmer, S. M.; Que, L., Jr.; Salowe, S. P.; Stubbe, J. *J. Am. Chem. Soc.* **1986**, *108*, 6832.

(26) Ericson, A.; Hedman, B.; Hodgson, K. O.; Green, J.; Dalton, H.; Bentsen, J. G.; Beer, R. H.; Lippard, S. J. *J. Am. Chem. Soc.* **1988**, *110*, 2330.

(27) Averill, B. A.; Davis, J. C.; Burman, S.; Zirino, T.; Sanders-Loehr, J.; Loehr, T. M.; Sage, J. T.; Debrunner, P. G. *J. Am. Chem. Soc.* **1987**, *109*, 3760, and references therein.

(28) Mukherjee, R. N.; Abrahamson, A. J.; Patterson, G. S.; Stack, T. D. P.; Holm, R. H. *Inorg. Chem.* **1988**, *27*, 2137.

(29) Tsumaki, T.; Antoku, S.; Shito, M. *Bull. Chem. Soc. Jpn.* **1960**, *33*, 1096.

(30) Tsumaki, T. *Bull. Chem. Soc. Jpn.* **1935**, *10*, 74.

the crystal structures of the three oxidation levels, allowing for the first time structural comparisons of fully oxidized and reduced and mixed-valence binuclear Fe complexes.

Experimental Section

Preparation of Compounds. The Schiff base H_3salmp[5] (**4**) was prepared by a published method.[31] The Duff reaction[32] was used to prepare 4- and 5-methylsalicylaldehydes, which were employed in the synthesis of methyl-substituted derivatives of **4** required for NMR signal assignments of Fe complexes. The following preparations were carried out under a pure dinitrogen atmosphere unless otherwise noted. Solvents were appropriately dried and degassed prior to use.

Fe_2(salmp)$_2$·2DMF (6). This compound was obtained by modification of an earlier procedure;[29] the preparation was performed without exclusion of air. To a suspension of 4.0 g (12 mmol) of H_3salmp in 250 mL of ethanol at 70 °C was added a filtered solution of 1.2 g (7.4 mmol) of anhydrous $FeCl_3$ in 100 mL of ethanol. This mixture was treated with a solution of 2.5 g (25 mmol) of triethylamine in 50 mL of ethanol, and the suspension was stirred for 2 h at 70 °C. The solid isolated by filtration of the reaction mixture was recrystallized from boiling DMF to yield 2.4 g (68%) of the pure product as a red-brown microcrystalline solid, sparingly soluble in DMF and insoluble in most common organic solvents. Anal. Calcd for $C_{48}H_{44}Fe_2N_6O_8$: C, 61.03; H, 4.69; Fe, 11.82; N, 8.90. Found: C, 61.12; H, 4.67; Fe, 12.07; N, 8.94. Absorption spectrum (DMF) λ_{max} (ϵ_M) 324 (26 800), 356 (sh, 21 400), 434 (6640), 488 (5900) nm. This compound as a solid and in solution is air-stable; it forms red-brown solutions.

$(Et_4N)_2$[Fe_2(salmp)$_2$] (7). Method A. To a stirred suspension of 2.08 g (6.00 mmol) of H_3salmp in 15 mL of methanol was added 10.2 g of a 26.2% solution of Et_4NOH in methanol (18.2 mmol of base). The yellow solution was stirred for 30 min, and the solvent was removed in vacuo. The oily residue was triturated with a small quantity of dry THF, which was then removed. The oil was partially dissolved in 40 mL of acetonitrile, and the slurry was treated with 0.98 g (6.00 mmol) of $FeCl_2$·$2H_2O$ to afford a dark blue-green mixture. After being stirred for 2 h, the reaction mixture was filtered, and 60 mL of ether was added to the filtrate. A dark microcrystalline solid was collected by filtration after 2 days. It was recrystallized from acetonitrile/ether and dried in vacuo to yield 0.80 g (25%) of pure product as a blue-green microcrystalline solid. Anal. Calcd for $C_{58}H_{70}Fe_2N_6O_6$: C, 65.79; H, 6.66; Fe, 10.55; N, 7.94. Found: C, 64.80; H, 6.69; Fe, 10.36; N, 7.59. Absorption spectrum (DMF) λ_{max} (ϵ_M) 380 (32 100), 600 (sh, 2920), 644 (3640), 800 (sh, 1010). The compound is extremely air-sensitive; it forms blue-green solutions.

Method B. A solution prepared from 0.178 g (1.17 mmol) of acenaphthylene and excess sodium (0.030 g, 1.30 mg atom) in THF was filtered into a suspension of 0.50 g (0.53 mmol) of Fe_2(salmp)$_2$·2DMF in 25 mL of DMF. After the reaction mixture was stirred for 2 h, THF was removed in vacuo, the mixture was filtered, and 0.194 g (1.17 mmol) of Et_4NCl was added to the filtrate. This solution was stirred overnight, NaCl was removed by filtration, and the filtrate was layered with 50 mL of ether. The mixture was allowed to stand overnight and then filtered, and the solid material was recrystallized from acetonitrile/ether to afford 0.37 g (67%) of pure product. This material is spectroscopically identical with that prepared by method A.

(Et_4N)[Fe_2(salmp)$_2$] (8). Method A. To a solution of $(Et_4N)_2$[Fe_2(salmp)$_2$] in 25 mL of acetonitrile was added 0.47 g (0.50 mmol) of Fe_2(salmp)$_2$·2DMF. The green-brown solution was stirred for 3 h and filtered to remove any unreacted starting material. Addition of 75 mL of ether resulted in the separation of a solid over a 2-day period. This material was collected and recrystallized from acetonitrile/ether to afford, after drying in vacuo, 0.51 g (55%) of pure product as a brown microcrystalline solid. Anal. Calcd for $C_{50}H_{50}Fe_2N_5O_6$: C, 64.67; H, 5.43; Fe, 12.03; N, 7.54. Found: C, 64.52; H, 5.65; Fe, 11.65; N, 7.68. Absorption spectrum (DMF) λ_{max} (ϵ_M) 373 (22 800), 425 (sh, 6860), 464 (sh, 4310), 588 (sh, 1960), 1295 (590) nm. The compound is air-sensitive; it forms deep red-brown solutions.

Method B. To a suspension of 0.50 g (0.53 mmol) of Fe_2(salmp)$_2$·2DMF in 25 mL of methanol was added 0.086 g (0.53 mmol) of $(Et_4N)SH$. The resulting black-green solution was stirred for 2 h, filtered, and concentrated in vacuo to about 10 mL. To this solution was added 25 mL of ether, causing separation of a solid overnight. This material was collected and recrystallized from acetonitrile/ether to give 0.35 g (60%) of product, whose spectroscopic properties are identical with those of the product of method A.

(31) Kambe, S.; Takajo, T.; Saito, K.; Hayashi, T.; Sakurai, A.; Midorikawa, H. *Synthesis* **1975**, 802.
(32) Duff, J. C. *J. Chem. Soc.* **1941**, 547.

Table I. Crystallographic Data[a] for Fe_2(salmp)$_2$·2DMF (**6**), $(Et_4N)_2$[Fe_2(salmp)$_2$]·4MeCN (**7**·4MeCN), and (Et_4N)[Fe_2(salmp)$_2$]·2DMF (**8**·2DMF)

	6	**7**·4MeCN	**8**·2DMF
formula	$C_{48}H_{44}Fe_2N_6O_8$	$C_{66}H_{82}Fe_2N_{10}O_6$	$C_{56}H_{64}Fe_2N_7O_8$
formula wt	944.05	1222.35	1074.89
a, Å	9.907 (5)	18.248 (5)	12.669 (3)
b, Å	10.584 (6)	15.454 (6)	12.992 (2)
c, Å	20.709 (6)	23.321 (6)	16.928 (4)
α			99.27 (2)
β	93.28 (3)	96.64 (3)	101.54 (2)
γ			95.91 (2)
V, Å^3	2178 (2)	6532 (3)	2668 (1)
Z	2	4	2
space group	$P2_1/c$	$P2_1/c$	$P\bar{1}$
ρ_{calcd} (ρ_{obsd}), g/cm^3	1.45 (1.44)	1.31 (1.29)	1.34 (1.33)
μ, cm^{-1}	7.3	4.9	6.0
$R(F_o)$	4.35	8.18	7.66
$R_w(F_o)$	5.63	11.3	8.24

[a] T = 297 K, λ = 0.710 69 Å (Mo Kα).

Collection and Reduction of X-ray Data. Single crystals of **6** were obtained by slow cooling of a warm DMF solution, while single crystals of **7**·4MeCN and **8**·2DMF were grown by vapor diffusion of ether into concentrated acetonitrile and DMF solutions, respectively. A black, hexagonal-shaped crystal of **6** and irregularly shaped crystals of **7**·4MeCN and **8**·2DMF were mounted in glass capillaries under a dinitrogen atmosphere. Data collection was carried out at ambient temperature on a Nicolet P3F automated four-circle diffractometer equipped with a graphite monochromator. Unit cell parameters were obtained from 25 machine-centered reflections ($20° \leq 2\theta \leq 25°$). Intensities of three check reflections monitored every 123 reflections indicated no significant decay in intensities over the course of the data collections. Data sets were processed with the program XTAPE of the SHELXTL program package (Nicolet XRD Corporation, Madison, WI 53711), and empirical absorption corrections were applied using the programs XEMP (**6**) and PSICOR (**7**·4MeCN, **8**·2DMF). For **6** and **7**·4MeCN, axial photographs and the observed systematic absences $h0l$, $00l$ ($l = 2n + 1$), and $0k0$ ($k = 2n + 1$) are consistent with the space group $P2_1/c$. For **8**·2DMF, axial photographs and the lack of systematic absences were consistent with the space groups $P1$ or $P\bar{1}$. Simple E statistics indicated the centrosymmetric space group as the correct choice. Subsequent structure solutions and refinements corroborated the choice of space groups. Crystallographic data for the three compounds are summarized in Table I.[33]

Structure Solution and Refinement. Atom scattering factors were taken from a standard source.[34] For the three compounds the Fe atoms and the atoms in the coordination spheres were located by direct methods using the program MULTAN. All carbon atoms were located in successive Fourier maps and were refined by using the program CRYSTALS. Isotropic refinement converged at the conventional R values of 11.3% (**6**), 15.0% (**7**·4MeCN), and 9.5% (**8**·2DMF). All atoms in **6** were treated anisotropically. In **7**·4MeCN, all atoms in the anion were refined anisotropically; owing to data limitations, all other atoms were treated isotropically. Furthermore, one cation in **7**·4MeCN was found to have disordered methylene carbon atoms, and each of the four acetonitrile solvate molecules to possess large thermal parameters indicative of some disorder. In **8**·2DMF, only the two Fe atoms and the N and O atoms of their coordination spheres were treated anisotropically because of limitations in the number of data. Attempts to describe the entire anion anisotropically by inclusion of low-intensity data increased the esd's by 10–20%. Hydrogen atoms were included on well-ordered carbon atoms in the final stages of refinement at 0.95 Å from, and with thermal parameters 1.2× those of, bonded carbon atoms. Final R values are given in Table I; atom positional and thermal parameters have been deposited as supplementary material.[33]

Other Physical Measurements. All measurements were performed under strictly anaerobic conditions. Absorption spectra were determined on a Perkin-Elmer Lambda 4C or a Cary 219 spectrophotometer. ^{1}H NMR spectra were recorded on a Brüker AM-250 spectrometer with an internal Me_4Si standard. Magnetic susceptibility measurements of solids were performed at an applied field of 5 kOe on a SHE SQUID magnetometer operating between 6 and 300 K. Measurements were made on

(33) See the paragraph at the end of this article concerning supplementary material.
(34) Cromer, D. T.; Waber, J. T. *International Tables for X-Ray Crystallography*; Kynoch Press: Birmingham, England, 1974.

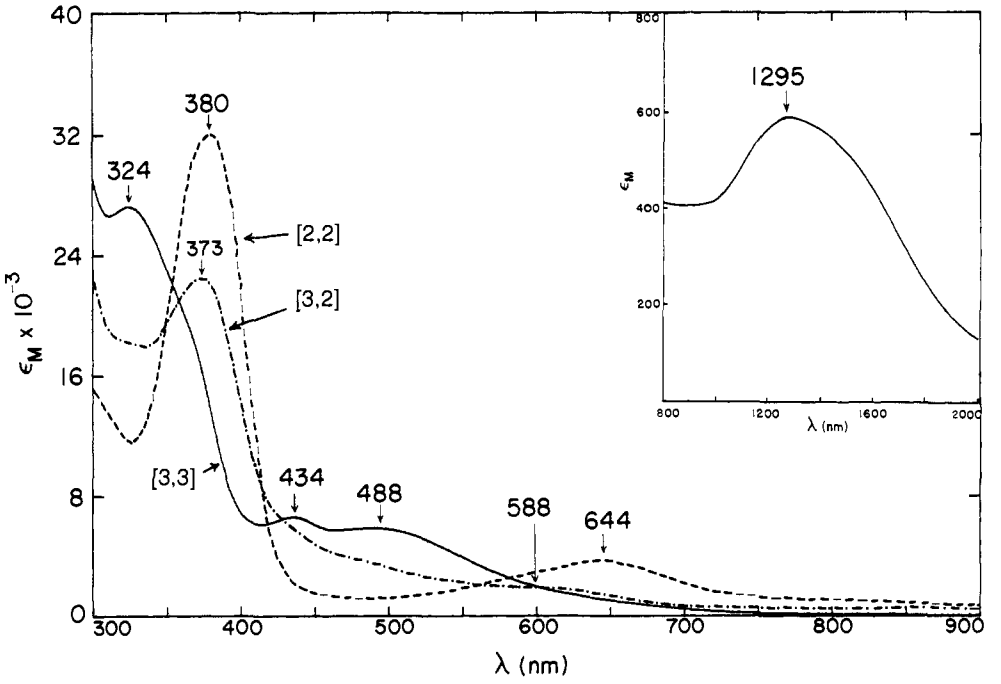

Figure 2. Absorption spectra of $Fe_2(salmp)_2$ = [3,3], $[Fe_2(salmp)_2]^{1-}$ = [3,2], and $[Fe_2(salmp)_2]^{2-}$ = [2,2] in DMF solutions. Inset: near-IR region of the spectrum of [3,2] showing the intervalence band.

finely ground polycrystalline samples loaded into precalibrated containers and sealed with epoxy resin under a dinitrogen/helium atmosphere. Compound **6** was measured as its bis(DMF) solvate. Compounds **7** and **8** were measured in unsolvated forms. The solvated forms of these compounds desolvate so readily that solid-state magnetic measurements on them are not feasible. Diamagnetic susceptibility corrections were applied. Solution susceptibilities were determined by the usual NMR method;[35] solvent susceptibilities were literature values.[36] Electrochemical experiments were carried out with standard PAR instrumentation, with use of a Pt working electrode, a SCE reference electrode, and 0.1 M $(n\text{-}Bu_4N)ClO_4$ supporting electrolyte in DMF solutions.

Results and Discussion

Preparation and Properties of $[Fe_2(salmp)_2]^{0,1-,2-}$. In the report of the preparation of the Fe(III) complex with salmp in 1960,[29] it was stated that a quantitative yield of the product Fe(salmp) could be obtained by the reaction of ligand **4** with $FeCl_3$ in hot ethanol. We have been unable to reproduce that result but have found that inclusion of base as in reaction 1 permits isolation in 68% yield of the product as a brown solid which has the binuclear formulation $Fe_2(salmp)_2$, proven by X-ray crystallography.

$$2FeCl_3 + 2H_3salmp + 6Et_3N \rightarrow Fe_2(salmp)_2 + 6Et_3NHCl \quad (1)$$

$Fe_2(salmp)_2$ is practically insoluble in most common solvents but is sufficiently soluble in DMF to allow measurement of its absorption spectrum, given in Figure 2, and its coulometry and cyclic voltammetry. The latter, shown in Figure 3, reveals two chemically reversible redox steps (i_{pc}/i_{pa} = 1) with $E_{1/2}$ = −0.46 and −1.00 V vs SCE. Controlled-potential coulometry demonstrated that each step is a one-electron process. No reversible oxidation steps were observed. Thus, $Fe_2(salmp)_2$ is the terminal oxidized member of the three-membered electron-transfer series (2). The reduced members of the series when isolated and examined (vide infra) show the same potentials and n values within experimental error, verifying that the two redox steps are reversible.

$$\underset{2Fe(III)}{[Fe_2(salmp)_2]} \xleftrightarrow{-0.46\ V} \underset{Fe(III)\cdot Fe(II)}{[Fe_2(salmp)_2]^{1-}} \xleftrightarrow{-1.00\ V} \underset{2Fe(II)}{[Fe_2(salmp)_2]^{2-}} \quad (2)$$

(35) Live, D. H.; Chan, S. I. *Anal. Chem.* **1970**, *42*, 791.
(36) Gerger, W.; Mayer, U.; Gutmann, V. *Monatsh. Chem.* **1977**, *108*, 417.

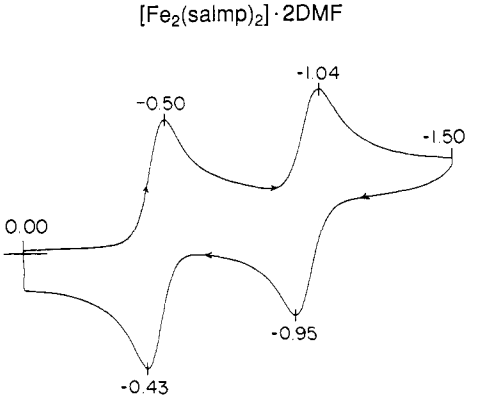

Figure 3. Cyclic voltammogram of $Fe_2(salmp)_2$ in DMF at 50 mV/s; peak potentials vs SCE are indicated.

The fully reduced member $[Fe_2(salmp)_2]^{2-}$ was prepared by reactions 3 and 4 and isolated as the highly dioxygen-sensitive Et_4N^+ salt. The yield of reaction 4 (67%) was significantly better. The mixed-valence member $[Fe_2(salmp)_2]^{1-}$ was obtained by reduction reaction 5 and the comproportionation reaction 6 in yields of 55–60%, also as the Et_4N^+ salt. For the latter, log K_{com} = $[E(0/1-) - E(1-/2-)]/0.059$ and $K_{com} = 1.4 \times 10^9$, showing negligible disproportionation of the product.

$$2FeCl_2 + 2(Et_4N)_3(salmp) \rightarrow (Et_4N)_2[Fe_2(salmp)_2] + 4(Et_4N)Cl \quad (3)$$

$$Fe_2(salmp)_2 + 2NaC_{12}H_8 \rightarrow Na_2[Fe_2(salmp)_2] + 2C_{12}H_8 \quad (4)$$

$$Fe_2(salmp)_2 + HS^- \rightarrow [Fe_2(salmp)_2]^{1-} + \tfrac{1}{2}H_2S_2 \quad (5)$$

$$Fe_2(salmp)_2 + [Fe_2(salmp)_2]^{2-} \rightleftharpoons 2[Fe_2(salmp)_2]^{1-} \quad (6)$$

Each of the complexes is readily identified by its UV–visible absorption spectrum (Figure 2), which is dominated by $RO^- \rightarrow$ Fe charge-transfer bands. The feature at 800 nm (sh, ϵ_M 1010, not clearly evident in the figure) in the spectrum of $[Fe_2(salmp)_2]^{2-}$ is assigned to a transition of octahedral $^5T_{2g} \rightarrow {}^5E_g$ parentage. The most conspicuous feature of the spectrum of $[Fe_2(salmp)_2]^{1-}$ is the broad band at λ_{max} (ϵ_M) = 1295 (590) nm. This is assigned to an intervalence transition, suggesting that the monoanion conforms to a type II mixed-valence complex in the Robin–Day classification.[37] On the Mössbauer time scale, $[Fe_2(salmp)_2]^{1-}$

Table II. Electrochemical and Magnetic Properties of $[Fe_2(salmp)_2]^{0,1-,2-}$ Complexes

property	$Fe_2(salmp)_2$	$[Fe_2(salmp)_2]^{1-}$	$[Fe_2(salmp)_2]^{2-}$
$E_{1/2}$, V (ΔE_p, mV)[a,b]	−0.46 (70)	−0.45 (70)	−0.46 (70)
	−1.00 (90)	−0.98 (80)	−0.99 (80)
n[c] (process)[a]	1.03 (0→1−)		0.96 (2−→1−)
	0.95 (1−→0)		0.97 (1−→2−)
J; zJ', cm^{-1}	1.21; −0.018	8.6; 0	1.23; 0
C, emu K/mol	8.41	11.3	10.7
T range, K	60–302	6–25	6–19
θ, K	9.6	−0.12	−0.86
μ_{eff}, μ_B			
solid[d]	8.20	9.50	9.22
solid (300 K)	8.33	7.96	8.19
MeCN (300 K)	e	8.33	7.72

[a] DMF. [b] 50 mV/s. [c] F/mol dimer. [d] Average moment in specified Curie–Weiss regions. [e] Insufficiently soluble for measurement.

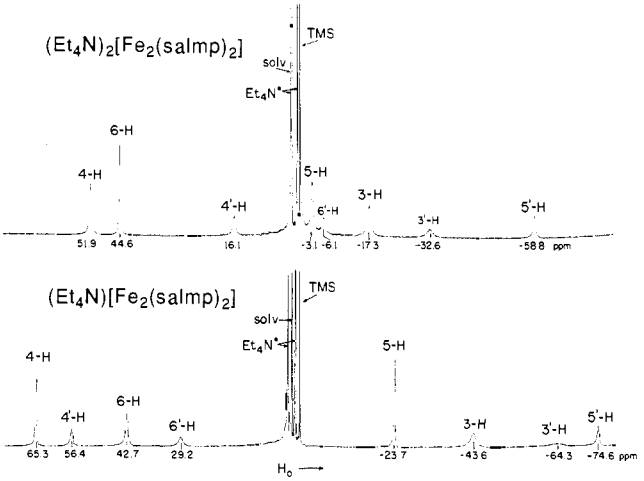

Figure 4. ^{1}H NMR spectra of $[Fe_2(salmp)_2]^{1-}$ and $[Fe_2(salmp)_2]^{2-}$ in CD_3CN solutions at 297 K; signal assignments are indicated.

in the solid state and in acetonitrile solution is a trapped-valence species up to 100 K.[38]

The complexes $[Fe_2(salmp)_2]^{1-,2-}$ are strongly paramagnetic in solution (Table II) and exhibit well-resolved, isotropically shifted ^{1}H NMR spectra, as shown for acetonitrile solutions in Figure 4. Similar spectra were observed in Me_2SO solutions. The spectrum of $Fe_2(salmp)_2$ was not obtained because of low solubility and large line widths arising from high-spin Fe(III). Signal assignments were made on the basis of relative line widths and intensities and methyl substitution at the 4/4′ and 5/5′ positions of the phenyl rings. That the shifts are dominantly contact[39] in origin follows from their alternating signs around the rings which are odd-alternate systems. The signs themselves are consistent with ligand → metal antiparallel spin transfer, a delocalization mode observed in other salicylaldiminate complexes of metals with incompletely filled dπ orbitals.[40,41] The only exception to this behavior is the 6′-H resonance in $[Fe_2(salmp)_2]^{2-}$, which experiences an isotropic shift of +13 ppm compared to −9 ppm for the 4′-H signal. Spectra of both complexes are consistent with their solid-state structures (vide infra) in that the four salicylideneamino and the two bridging phenolate groups are equivalent. For $[Fe_2(salmp)_2]^{1-}$, intramolecular electron exchange is fast on the NMR time scale.

Structures of $[Fe_2(salmp)_2]^{0,1-,2-}$. While the salmp ligand **4** apparently cannot accommodate mononuclear five-coordination,

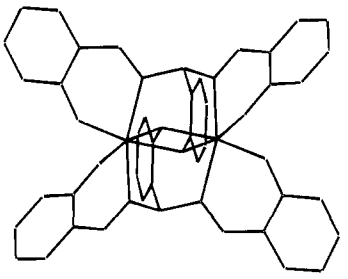

$[Fe_2(salmp)_2]^{0,1-,2-}$ (6-8)

Figure 5. Depiction of the ligand conformation in $[Fe_2(salmp)_2]^{0,1-,2-}$, which is practically invariant over the three structures.

at least with metal ions of the sizes found in the first transition series, it is estimably suited to form binuclear complexes. In the arrangement encountered here, the six oxygen atoms of two ligands are roughly coplanar with the two Fe atoms, which experience distorted octahedral coordination. The two octahedra share a common edge and are bridged by two phenolate oxygen atoms; terminal coordination in the plane is fulfilled by salicylideneamino oxygen atoms. Within each octahedron, coordination is completed by two trans nitrogen atoms. Consequently, each ligand generates four six-membered chelate rings. Under this arrangement, there are three possible isomers: C_{2h}, with the two terminal oxygens cis or trans to the bridging oxygen of the *same* ligand; C_2, with one oxygen cis and the other trans to the bridging oxygen of the same ligand.

The trans-C_{2h} structure is that adopted by all three complexes $[Fe_2(salmp)_2]^{0,1-,2-}$ (**6–8**). This conformation is illustrated

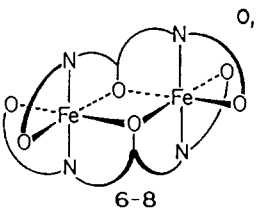

schematically here for simplicity and more exactly in Figure 5. The structures of the $Fe_2O_6N_4$ coordination units of the three complexes, containing the bridge unit **5**, are presented in Figure 6. Selected interatomic distances and angles are contained in Table III. Having established the invariant conformation of the ligand, the remaining matters of interest are comparative structural details over the three oxidation levels. Some dimensional variations are expected inasmuch as the Shannon radii[42] for high-spin, six-coordinate Fe(III) and Fe(II) are 0.79 and 0.92 Å, respectively. We observe that the structures of the Et_4N^+ salts of $[Fe_2(salmp)_2]^{1-,2-}$, while adequate for comparison, are not as highly refined as that of $Fe_2(salmp)_2$ because of the difficulties in obtaining crystals of high diffraction quality and of disorder in cation and solvate in the dianionic compound. $Fe_2(salmp)_2$ and $[Fe_2(salmp)_2]^{1-}$ have crystallographically imposed centrosymmetry, and the latter occurs as two independent half-anions in the asymmetric unit. No symmetry is imposed on $[Fe_2(salmp)_2]^{2-}$. Metric data quoted below are mean values when there is more than one independent value for a given type of distance or angle. Such values are included in Figure 6 and are useful for examining trends in structural parameters.

Terminal Fe–O bonds increase in length as the extent of reduction increases, i.e., along series 2, the difference being 0.07–0.08 Å between oxidation levels. The same effect holds for bridging Fe–O distances, with differences of 0.05–0.07 Å. However, the Fe–N bonds increase much less upon reduction, from 2.15 to 2.18 Å, an effect that arises because of constraints on the position of the nitrogen atoms by tight binding of the anionic oxygen atoms that anchor four rigid six-membered chelate rings.

(37) Robin, M. D.; Day, P. *Adv. Inorg. Chem. Radiochem.* **1967**, *10*, 247.
(38) Surerus, K. K.; Münck, E.; Snyder, B. S.; Holm, R. H. *J. Am. Chem. Soc.*, in press.
(39) $(\Delta H/H_0)_{iso} = (\Delta H/H_0)_{dia} - (\Delta H/H_0)_{obsd} = (\Delta H/H_0)_{con} + (\Delta H/H_0)_{dipolar}$.
(40) Horrocks, W. D., Jr. In *NMR of Paramagnetic Molecules: Principles and Applications*; La Mar, G. N.; Horrocks, W. D., Jr.; Holm, R. H., Eds.; Academic Press: New York, 1973; Chapter 4.
(41) La Mar, G. N.; Eaton, G. R.; Holm, R. H.; Walker, F. A. *J. Am. Chem. Soc.* **1973**, *95*, 63.
(42) Shannon, R. D. *Acta Crystallogr.* **1976**, *A32*, 751.

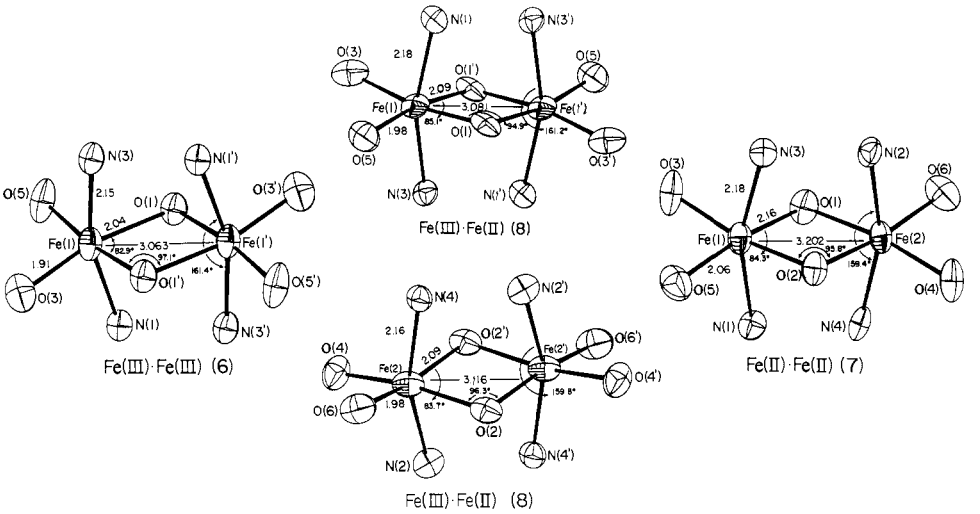

Figure 6. Structures of the coordination units of $Fe_2(salmp)_2$ (**6**), $[Fe_2(salmp)_2]^{1-}$ (**8**·2DMF), and $[Fe_2(salmp)_2]^{2-}$ (**7**·4MeCN), showing 50% probability ellipsoids and the atom labeling schemes. The indicated bond angles and distances are *mean* values when a given distance or angle type has more than one independent value.

Table III. Selected Interatomic Distances (angstroms) and Angles (degrees) in $[Fe_2(salmp)_2]$·2DMF (**6**), $(Et_4N)_2[Fe_2(salmp)_2]$·4MeCN (**7**·4MeCN), and $(Et_4N)[Fe_2(salmp)_2]$·2DMF (**8**·2DMF)

	6[a]	**8**·2DMF[a]	**7**·4MeCN	
		Bridge		
Fe(1)–O(1)	2.023 (2)	2.102 (8)	Fe(1)–O(1)	2.168 (8)
Fe(2)–O(2)		2.068 (8)	Fe(1)–O(2)	2.129 (7)
Fe(1)–O(1′)	2.064 (2)	2.079 (9)	Fe(2)–O(1)	2.145 (8)
Fe(2)–O(2′)		2.115 (8)	Fe(2)–O(2)	2.195 (7)
Fe(1)–N(1)	2.156 (3)	2.177 (10)	Fe(1)–N(1)	2.196 (9)
Fe(2)–N(2)		2.177 (10)	Fe(1)–N(3)	2.188 (9)
Fe(1)–N(3)	2.138 (3)	2.180 (10)	Fe(2)–N(2)	2.162 (9)
Fe(2)–N(4)		2.158 (10)	Fe(2)–N(4)	2.156 (9)
Fe(1)–Fe(1′)	3.063 (1)	3.081 (4)	Fe(1)–Fe(2)	3.202 (2)
Fe(2)–Fe(2′)		3.116 (4)		
O(1)–O(1′)	2.707 (4)	2.826 (17)	O(1)–O(2)	2.898 (10)
O(2)–O(2′)		2.791 (15)		
Fe(1)–O(1)–Fe(1′)	97.06 (9)	94.9 (4)	Fe(1)–O(1)–Fe(2)	95.9 (3)
Fe(2)–O(2)–Fe(2′)		96.3 (3)	Fe(1)–O(2)–Fe(2)	95.6 (3)
O(1)–Fe(1)–O(1′)	82.94 (9)	85.1 (4)	O(1)–Fe(1)–O(2)	84.8 (2)
O(2)–Fe(2)–O(2′)		83.7 (3)	O(1)–Fe(2)–O(2)	83.8 (2)
N(1)–Fe(1)–O(1)	82.5 (1)	85.4 (3)	N(1)–Fe(1)–O(1)	83.6 (3)
N(2)–Fe(2)–O(2)		81.7 (3)	N(1)–Fe(1)–O(2)	81.4 (3)
N(1)–Fe(1)–O(1′)	81.8 (1)	82.8 (3)	N(3)–Fe(1)–O(1)	80.5 (3)
N(2)–Fe(2)–O(2′)		81.0 (3)	N(3)–Fe(1)–O(2)	82.5 (3)
N(3)–Fe(1)–O(1)	86.9 (1)	83.0 (3)	N(2)–Fe(2)–O(1)	83.0 (3)
N(4)–Fe(2)–O(2)		85.7 (3)	N(2)–Fe(2)–O(2)	83.4 (3)
N(3)–Fe(1)–O(1′)	81.8 (1)	81.5 (3)	N(4)–Fe(2)–O(1)	83.7 (3)
N(4)–Fe(2)–O(2′)		81.9 (3)	N(4)–Fe(2)–O(2)	81.0 (3)
N(1)–Fe(1)–N(3)	161.4 (1)	161.2 (4)	N(1)–Fe(1)–N(3)	158.3 (3)
N(2)–Fe(2)–N(4)		159.8 (4)	N(2)–Fe(2)–N(4)	160.4 (3)
		Terminal		
Fe(1)–O(3)	1.894 (3)	1.961 (9)	Fe(1)–O(3)	2.040 (8)
Fe(2)–O(4)		1.970 (8)	Fe(1)–O(5)	2.080 (8)
Fe(1)–O(5)	1.921 (3)	1.991 (9)	Fe(2)–O(4)	2.047 (8)
Fe(2)–O(6)		1.994 (9)	Fe(2)–O(6)	2.059 (8)
O(5)–Fe(1)–O(1)	91.6 (1)	94.0 (4)	O(1)–Fe(1)–O(3)	94.0 (3)
O(6)–Fe(2)–O(2)		93.2 (4)	O(2)–Fe(1)–O(5)	97.3 (3)
O(3)–Fe(1)–O(1′)	93.4 (1)	92.5 (4)	O(3)–Fe(1)–O(5)	86.4 (4)
O(4)–Fe(2)–O(2′)		95.0 (3)	O(1)–Fe(2)–O(6)	95.8 (3)
O(3)–Fe(1)–O(5)	93.6 (1)	90.4 (4)	O(2)–Fe(2)–O(4)	95.1 (3)
O(4)–Fe(2)–O(6)		90.2 (4)	O(4)–Fe(2)–O(6)	87.0 (4)

[a] Primed and unprimed atoms related by an inversion center.

In the centrosymmetric cases, the Fe_2O_2 portions of bridge units **5** are planar rhombs with markedly unequal Fe–O distances and acute O–Fe–O (83–85°) and obtuse Fe–O–Fe (95–97°) angles. For example, these distances differ by 0.041 Å in $Fe_2(salmp)_2$. In this complex and $[Fe_2(salmp)_2]^{1-}$, bridging phenolate rings are exactly parallel and virtually normal to the Fe–Fe vectors. However, the ligand conformation in $[Fe_2(salmp)_2]^{2-}$ is less regular, placing the two bridging phenolate rings at an interplanar angle of 178° to each other and at angles of 86.8° and 94.1° to the Fe–Fe vector. This is clearly reflected in the even less regular bridge unit structure of this complex which, nonetheless, retains a planar Fe_2O_2 rhomb. In addition to the Fe–O bonds, the Fe···Fe (3.06–3.20 Å) and O···O (2.71–2.90 Å) separations increase across series 2. The N–Fe–N angles (158–161°) deviate considerably

from linearity owing to constraints of the N-C-N portion of **5** in which the angles at carbon (106-110°) are slightly strained. These angular parameters change only slightly and not monotonically as the oxidation level decreases. Overall, bond-length changes are consistent with the larger size of Fe(II) over Fe(III), and the dimensions of the Fe_2O_2 unit expand accordingly with small angular changes. Indeed, differences in terminal (0.15 Å) and bridge (0.14 Å) Fe-O distances in $[Fe_2(salmp)_2]^{2-}$ and $Fe_2(salmp)_2$ are entirely comparable with the difference in Shannon radii (0.13 Å) of the two ions. Metric parameters of $[Fe_2(salmp)_2]^{1-}$ are approximate averages of the corresponding values in $[Fe_2(salmp)_2]^{0,2-}$. Because of imposed centrosymmetry, this complex does not exhibit structurally distinct Fe(II,III) sites.

Bond distances in the Fe(II,II) and Fe(III,III) complexes are unexceptional when compared to those in salicylaldiminato complexes. Terminal Fe-O and Fe-N bond distances in $[Fe_2(salmp)_2]^{2-}$ are slightly shorter than those of one five-coordinate Fe(II)-salen complex,[28] which is the only comparison available. The range of these bond distances overlap in five-[8,9c] and six-coordinate[12a,c,j,21,43] Fe(III) complexes, and the corresponding bond lengths of $Fe_2(salmp)_2$ occur in these ranges. The bridging Fe-O bond distances in the latter complex are very close to those of binuclear Fe(III) species containing one bridging phenolate group.[21]

Comparison with Other Binuclear Fe Complexes. Among complexes with bridge units **1-3**, the set $[Fe_2(salmp)_2]^{0,1-,2-}$ is unique in several interesting and significant respects, which are next considered.

(a) Ligand Topology. In this context, **4** is a unique binucleating pentadentate. It forms (actual or idealized) centrosymmetric *bis*-ligand complexes having doubly bridged (idealized) octahedral binding sites without requiring exogenous ligands. The closest approaches to this situation are found with the binuclear Fe complexes of the deprotonated heptadentates saltrien (**9**), hxta (**10**), and bpmp (**11**), each of which contains an endogenous bridging phenolate group. The ligand bzim (not shown), which also forms a binuclear phenolate-bridged Fe complex,[18a] differs from **11** in having 2-benzimidazolylmethyl instead of 2-pyridyl groups. Ligand **9** has been known for some time,[44] but its Fe(III)

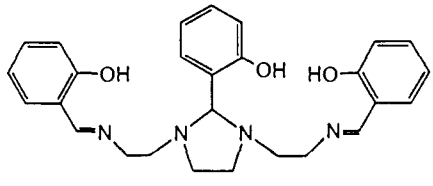

9

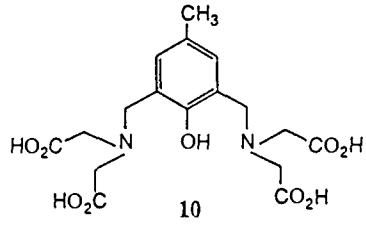

10

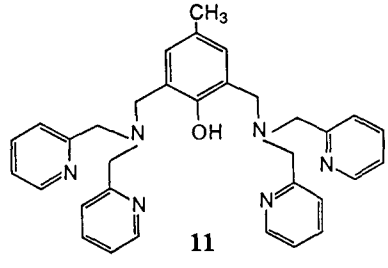

11

complexes have been isolated only relatively recently.[21] These are of the type $Fe_2(saltrien)(OR)Cl_2$ and contain bridge unit **2b**. Complexes of **10** and **11** prepared and examined by Que and co-workers,[12h,i,17,18b,19] are of the types $Fe_2(hxta)(OH)(OH_2)_2$ (**2b**), $[Fe_2(hxta)(RCO_2)_2]^{1-}$ (**3b**), and $[Fe_2(bpmp)(RCO_2)_2]^{3+}$ (**3b**) and incorporate the indicated bridge units.

(b) Bridge Structure. The structures of some 16 compounds containing the $Fe^{III}_2(OR)_2$ bridge in **2b** or **3d** have been determined by X-ray analysis.[11,12,21] The Fe···Fe separations and Fe-O-Fe angles, without exception, fall into the ranges 3.08-3.22 Å and 100-111°, respectively. Actually, the large majority of distances are longer than 3.10 Å and angles are larger than 103°. In $Fe_2(salmp)_2$, these values (3.06 Å, 97°) are the *smallest* yet found for complexes with this generalized bridge. As will be seen, the bridge angle, as well as other geometric factors, may influence magnetic properties. The only previously structurally characterized $Fe^{II}_2(OR)_2$ bridge occurs in $[Fe_2L(Im)_4]^{2+}$,[13b] where L is a macrocyclic binucleating ligand with two phenolate bridges. The bridge angle of 96° is the same as that for $[Fe_2(salmp)_2]^{2-}$, but the Fe-O and Fe-Fe distances of 2.09 and 3.12 Å, respectively, are clearly shorter.

(c) Oxidation Levels. A conspicuously favorable feature of the salmp ligand is the stabilization of three oxidation levels in the form of reversible electron-transfer series 2, thereby allowing the isolation and structure determination of each. These three levels have been produced otherwise only in the series $[Fe_2(bpmp)(EtCO_2)_2]^{3+,2+,1+}$ having the potentials +0.69 and -0.01 V vs SCE.[19] These high values compared to those of series 2 are doubtless mainly due to the net positive charges of the complexes. The 2+ and 1+ complexes have been isolated, and their structures determined.[19] The highly positive potential of the 3+ species may make its isolation difficult. The $[Fe_2(hxta)(OAc)_2]^{1-,2-}$ potential is more negative (-0.29 V vs SCE), and both Fe(III,III) and Fe(III,II) complexes have been isolated.[17,18b]

In other cases for which some information is available, complexes containing bridge units **1a** and **3a** do not appear to form stable reduced species. Reduction products of μ-oxo Fe(III) porphyrins $[Fe(P)]_2O$ are obtainable at quite negative potentials but are readily cleaved by protic sources.[45] $[Fe_2O(Me_3tacn)_2(OAc)_2]^{2+}$ is reported to be reduced to a mixed-valence complex in a quasireversible process at -0.37 V vs SCE.[14c] The reduction product is unstable to disproportionation and was not isolated. The instability of these complexes arises because of the much enhanced basicity of the μ-oxo atom in molecules below the Fe(III,III) oxidation level, a matter underscored by the absence of any stable compound containing a Fe^{II}-O-Fe^{II} bridge.[46] Such basicity is effectively neutralized in RO^- bridge groups.

(d) Electron Delocalization. In addition to $[Fe_2(salmp)_2]^{1-}$, two other mixed-valence binuclear Fe complexes are known. $[Fe_2(hxta)(OAc)_2]^{2-}$[18b] and $[Fe_2(bpmp)(EtCO_2)_2]^{2+}$,[19] both with bridge unit **3b**, are trapped-valence at 55 K by the Mössbauer criterion. The structure of the latter, which is devoid of imposed symmetry, contains localized Fe(III) and Fe(II) sites. The intervalence bands of these complexes at 1275 (hxta) and 1340 nm (bpmp) and that of $[Fe_2(bzim)(PhCO_2)_2]^{2+}$ at 1400 nm[18a] are at energies comparable with that of $[Fe_2(salmp)_2]^{1-}$ (Figure 2). As with $[Fe_2(salmp)_2]^{1-}$, $[Fe_2(hxta)(OAc)_2]^{2-}$ is completely delocalized on the ^1H NMR time scale.[18b] In the context of electron delocalization, $[Fe_2(salmp)_2]^{1-}$ is unique only in that its Et_4N^+ salt crystallizes with centrosymmetry imposed on the anion.

(e) Magnetism. All complexes with the $Fe^{III}_2(OR)_2$ bridge as in units **2b** and **3d** are antiferromagnetic and show relatively weak spin coupling with J values ranging from ca. -5 to -20 cm^{-1}. These observations extend over more than 20 compounds.[11,12,13c,21b,47-52] The several examples of Fe(II,II) complexes with this bridge are

(43) Lauffer, R. B.; Heistand, R. H., II; Que, L., Jr. *Inorg. Chem.* **1983**, *22*, 50.

(44) (a) Mukherjee, A. K. *Sci. Cult.* **1953**, *19*, 107. (b) Das Sarma, B.; Bailar, J. C. *J. Am. Chem. Soc.* **1954**, *76*, 4052; **1955**, *77*, 5476.

(45) (a) Kadish, K. M.; Larson, G.; Lexa, D.; Momenteau, M. *J. Am. Chem. Soc.* **1975**, *97*, 282. (b) Kadish, K. M. *Prog. Inorg. Chem.* **1986**, *34*, 435.

(46) The converse of this statement is not true. There are examples of complexes with a hydroxyl bridge in the Fe(III,III) oxidation level, among them $Fe_2(saltrien)(OH)Cl_2$,[21b] $Fe_2(hxta)(OH)(OH_2)_2$,[12h,i] and $[Fe_2(HBpz_3)_2(OH)(OAc)_2]^{1+}$.[16b]

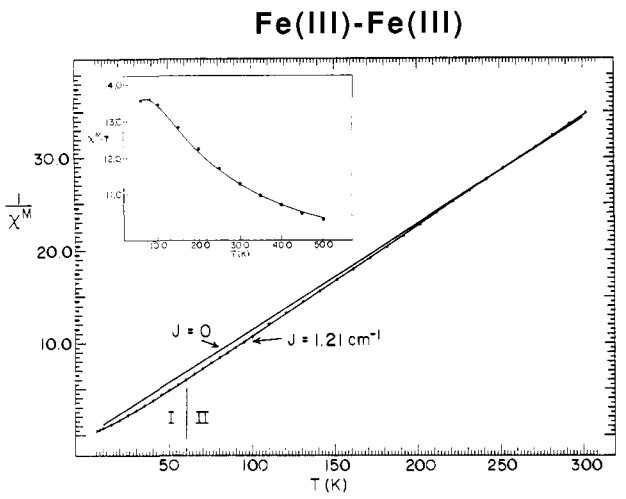

Figure 7. Temperature dependence of the reciprocal molar susceptibility of $Fe_2(salmp)_2$. In this and the following two figures, spin-uncoupled behavior is represented by the line $\chi^M = C/T$ ($J = 0$) plotted with the appropriate Curie constant in Table IV. The other line represents theoretical fits to the data in regions I and II using the parameters in Table II. The inset is an expanded view of the fit in region I showing $\chi^M T$ vs T.

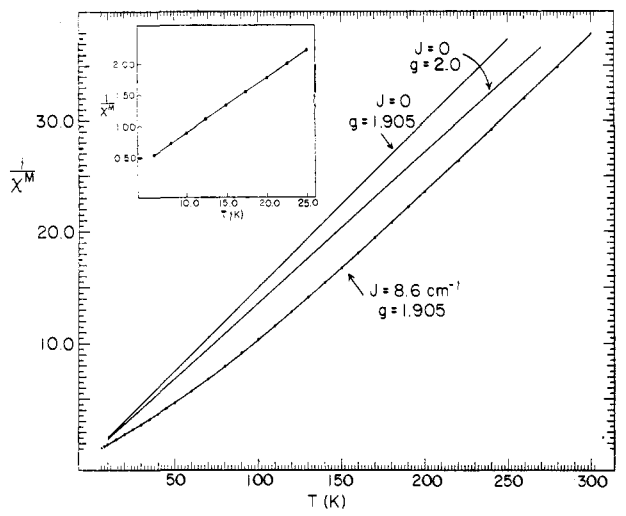

Figure 8. Temperature dependence of the reciprocal molar susceptibility of $[Fe_2(salmp)_2]^{1-}$. Spin-uncoupled behavior at two g values is illustrated. The remaining solid line is a theoretical fit to the data using the parameters in Table II. The inset is an expanded view of the Curie–Weiss fit to the low-temperature data.

also antiferromagnetic.[13a,b] As shown next, the complexes $[Fe_2(salmp)_2]^{0,1-,2-}$ are *ferromagnetic*.

Magnetic Properties. The magnetic susceptibilities of the set $[Fe_2(salmp)_2]^{0,1-,2-}$ have been determined over the interval 6–300 K. Plots of inverse molar susceptibility vs temperature are given in Figures 7–9. Each molecule has local spins S_1 and S_2 which, in the absence of antiferromagnetic behavior, may be noninteracting or coupled ferromagnetically to give ground-state spin $S = S_1 + S_2$. The temperature dependence of susceptibility is given by the van Vleck equation (7). Here J is the intramolecular

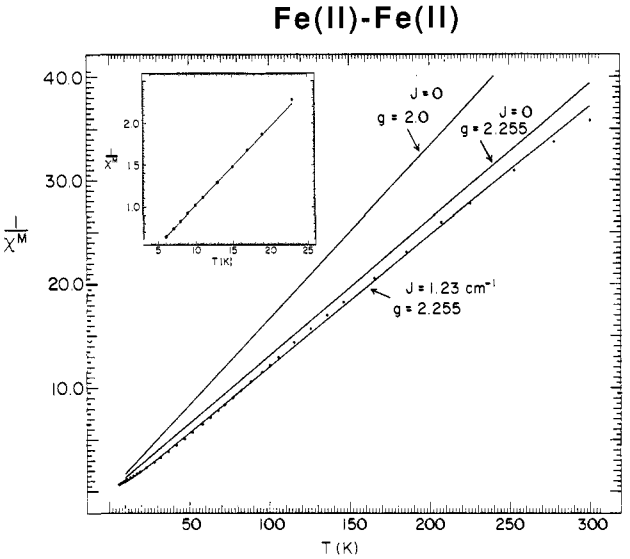

Figure 9. Temperature dependence of the reciprocal molar susceptibility of $[Fe_2(salmp)_2]^{2-}$. Spin-uncoupled behavior at two g values is illustrated. The remaining solid line is a theoretical fit to the data using the parameters in Table II. The inset is an expanded view of the Curie–Weiss fit to the low-temperature data.

Table IV. Calculated Magnetic Parameters for Two Uncoupled and Ferromagnetically Coupled High-Spin Fe Centers

S_1, S_2; $S = S_1 + S_2$	C,[a] emu K/mol	μ_{eff},[b] μ_B
Fe(III,III)		
$^5/_2, ^5/_2$	8.75	8.37
5	15	10.95
Fe(III,II)		
$^5/_2$, 2	7.375	7.68
$^9/_2$	12.375	9.95
Fe(II,II)		
2, 2	6	6.93
4	10	8.94

[a] Equation 8 ($g = 2$). [b] $\mu_{eff} = (3kC/N)^{1/2} = g[S(S+1)]^{1/2}\mu_B$ ($g = 2$).

$$\chi^M = Ng^2\mu_B^2 f(J,T)/kT \quad (7)$$

$$C = Ng^2\mu_B^2 S(S+1)/3k \quad (8)$$

exchange interaction in the Hamiltonian $H = -2JS_1 \cdot S_2$, whose eigenvalues are $E(S) = -J[S(S+1)]$, and the other symbols have their usual meaning. The functions $f(J,T)$, which are tabulated elsewhere,[53] are weighted sums of exponentials e^{nx}, where n is an integer and $x = J/kT$. In the event of Curie ($\chi^M = C/T$) or Curie–Weiss ($\chi^M = C/(T-\theta)$) behavior, the Curie constant C is given by eq 8. Magnetic constants for spin-isolated, and ferromagnetically coupled interactions of, Fe(III) and Fe(II) centers are collected in Table IV. Experimental magnetic results are included in Table II.

(a) $Fe_2(salmp)_2$. Magnetic data are plotted in Figure 7, from which it is immediately evident that the behavior below ca. 170 K departs from that of two independent Fe(III) centers ($J = 0$). While it was possible to obtain a reasonable fit of the experimental susceptibilities over the entire temperature range with eq 7 and $S_1 = S_2 = {}^5/_2$, the data in region I (6–60 K) were more satisfactorily treated by inclusion of an intermolecular term, $H' = -z'J'S_i \cdot S_j$, in the exchange Hamiltonian. Here z' is the lattice coordination number, J' is the intermolecular exchange energy, and the remaining terms are the spins of molecules i and j. The resultant expression for the susceptibility, eq 9,[54] when applied

$$\chi^M = Ng^2\mu_B^2 f(J,T)/[kT - 2z'J'f(J,T)] \quad (9)$$

(47) (a) Gerloch, M.; Lewis, J.; Mabbs, F. E.; Richards, A. *J. Chem. Soc. A* **1968**, 112. (b) Reiff, W. M.; Long, G. J.; Baker, W. A., Jr. *J. Am. Chem. Soc.* **1968**, *90*, 6347.
(48) Schugar, H. J.; Rossman, G. R.; Gray, H. B. *J. Am. Chem. Soc.* **1969**, *91*, 4564.
(49) Wu, C.-H.; Rossman, G. R.; Gray, H. B.; Hammond, G. S.; Schugar, H. J. *Inorg. Chem.* **1972**, *11*, 990.
(50) Wrobleski, J. T.; Brown, D. B. *Inorg. Chim. Acta* **1979**, *35*, 109.
(51) Borer, L. L.; Vanderbout, W. *Inorg. Chem.* **1979**, *18*, 526.
(52) Puri, R. N.; Asplund, R. O. *J. Coord. Chem.* **1981**, *11*, 73.
(53) O'Connor, C. J. *Prog. Inorg. Chem.* **1982**, *29*, 293.
(54) Ginsberg, A. P.; Lines, M. E. *Inorg. Chem.* **1972**, *11*, 2289.

to the data in region I, affords a fit with $J = 1.21$ cm^{-1} and $z'J' = -0.018$ cm^{-1}; i.e., intramolecular interactions are ferromagnetic and intermolecular interactions are very weak and antiferromagnetic. In the crystal, the distances from the centroid of the Fe_2O_2 bridge portion to the centroids of other unique molecules are 9.91–11.6 Å, and the shortest Fe–Fe separation is 8.39 Å.

In region II (60–300 K), the data closely correspond to Curie–Weiss behavior. The positive value of the Weiss constant is consistent with low-temperature ferromagnetism, and the Curie constant and magnetic moment are only slightly reduced from those expected for two uncoupled $S = {}^5/_2$ centers.

(b) $[Fe_2(salmp)_2]^{1-}$. As seen in Figure 8, the departure of this complex from uncoupled magnetic behavior is quite significant over the entire temperature range of measurement. The data were successfully analyzed under the exchange Hamiltonian with $S_1 = {}^5/_2$ and $S_2 = 2$ and with use of eq 7. The best fit to the data was obtained with $g = 1.905$ and $J = 8.6$ cm^{-1}. Intermolecular effects were neglected; the centroid–centroid distances are 10.3–13.0 Å, and the shortest Fe–Fe separation is 9.66 Å. In the 6–25 K range, Curie–Weiss behavior was observed with a Curie constant and magnetic moment indistinguishable from those expected for a $S = {}^9/_2$ ground state with $g = 1.905$ ($C = 11.2$, $\mu_{eff} = 9.48\mu_B$).

(c) $[Fe_2(salmp)_2]^{2-}$. The susceptibility data for this compound, presented in Figure 9, again deviate from the behavior of uncoupled spins. The most adequate treatment of the data utilized eq 7 with $S_1 = S_2 = 2$, $g = 2.255$, and $J = 1.23$ cm^{-1}, and a temperature-independent paramagnetic (TIP) contribution of 800 $\times 10^{-6}$ emu/mol. Again, intermolecular coupling was ignored. In this compound, the centroid–centroid distances of 11.9–13.9 Å are the largest in the set. At 6–19 K, the complex exhibits a well-defined Curie–Weiss region with a Curie constant and magnetic moment that approach the values for a $S = 4$ ground state with $g = 2.255$ ($C = 12.7$; $\mu_{eff} = 10.1$ μ_B). Agreement would be improved with a somewhat lower effective g value (Table IV). Although the data analysis over the entire temperature range is not as satisfactory as in the preceding two cases, the results establish a ferromagnetic interaction leading to a $S = 4$ ground state.

Magnetic moments of $[Fe_2(salmp)_2]^{1-,2-}$ in acetonitrile solution at 297 K are in reasonable agreement with those in the solid state at 300 K (Table II) and exceed by 0.6–0.8μ_B those expected for spin-uncoupled situations. Therefore, the existence of ferromagnetic interactions is an intrinsic molecular property of these complexes. The only other established binuclear ferromagnetic Fe compounds are mixed-valence $[Fe_2(OH)_3(Me_3tacn)_2]^{2+}$ [23] and $Cs_3[Fe_2F_9]$,[55] which have the common feature of face-shared octahedra.

Distortions and Orbital Energies. We have emphasized that, among complexes with a $Fe^{III}_2(OR)_2$ bridge as in **2b** and **3d**,[56] $Fe_2(salmp)_2$ is unique in being ferromagnetic. In general, bridge angles θ of 90°, which involve interactions of magnetic orbitals with orthogonal bridge atom p orbitals, will promote ferromagnetic behavior. Larger angles imply more bridge orbital s character and will favor antiferromagnetism. A crossover from ferromagnetism ($S = 1$) to antiferromagnetism ($S = 0$) has been observed in a series of complexes containing the $Cu^{II}_2(OH)_2$ bridge at $\theta \approx 98°$[57] and has been insightfully analyzed in the extended Hückel treatment of Hay et al.[58] Here the essential quantity is the energy separation between the two magnetic orbitals, which are of σ^* character, the larger separation favoring the singlet ground state. Because of the presence of 10 magnetic orbitals and a large number of magnetic exchange pathways, delineated by Ginsberg,[59] between bridged Fe(III) centers that are octahedral and high spin, any analyis of the transition from antiferromagnetic to ferromagnetic behavior will be difficult. Further, there is only a very small difference in exchange energies (<15 cm^{-1}) between a typical antiferromagnetic complex with bridge **2b** and $Fe_2(salmp)_2$. We have, however, attempted to identify structural factors that may contribute to the ferromagnetic ground state of $Fe_2(salmp)_2$ using the extended Hückel approach.

The calculational model is *trans*-$Fe_2(\mu_2\text{-}OH)_2(NH_3)_4(OH)_4$ (**12**),[60] which simulates the coordination environment of $Fe_2(salmp)_2$. In its idealized configuration, **12** has D_{2h} symmetry

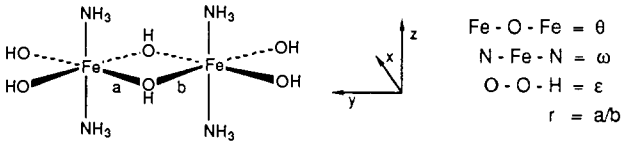

12

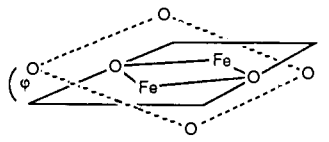

13

with $\theta = 90°$, other bond angles of 90°, and Fe–N/O bond distances that are the averages of those in Table III. The effects of certain geometric factors on the energies of the d-block orbitals are depicted in Figure 10. In the manner of Burdett[61] and Shaik et al.,[62] these orbitals may be derived from the interaction of linear combinations of $Fe(NH_3)_2(OH)_2$ fragment frontier orbitals with bridge s and p orbitals. The largest energy gap divides orbitals of the t_2 (lower) and e types (upper) of octahedral parentage; all are half-occupied in the ferromagnetic state. Variation of bridge angle θ from 90° to 110° mainly results in the stabilization of the b_{2u}, b_{2g}, and b_{3u} orbitals and destabilization of the a_g and lower b_{1u} orbitals. This behavior can be traced to changes in antibonding interactions of metal and bridge orbitals. At $\theta = 90°$, the energy difference between the lowest t_2 and lowest e level $\Gamma = 3.00$ eV and the t_2–e gap $\Delta = 2.23$ eV, while at $\theta = 110°$ $\Gamma = 2.93$ eV and $\Delta = 2.69$ eV. The behavior of Γ is opposite of what might be expected if smaller angles contribute to spin pairing; that of Δ suggests possible pairing of spins at larger values of θ. These results suggest that other geometric factors might be involved.

To generate the observed coordination stereochemistry of $Fe_2(salmp)_2$ from the idealized configuration of **12**, the following distortions are required: increase of θ to 96°; decrease of the N–Fe–N angle ω to 160°; displacement of terminal oxygen atoms from the bridge plane by the angle $\phi = 20°$ as shown in **13**; adjustment of bond distance ratio r from unity to 0.98. The effects of these distortions when carried out stepwise are also shown in Figure 10. An additional parameter, the O–O–H angle ϵ, was also explored and found to have a neglible effect; in all cases $\epsilon = 180°$. Under these distortions, the symmetry of the final configuration is C_i. For simplicity, orbitals are labeled according to their principal d component and as symmetric (s) or antisymmetric (a) to inversion. All orbitals are noticeably affected by the distortions. Changes in the orbital energy parameters are summarized as follows:

$\Gamma = 3.00$	3.05	2.68	2.72	2.60	eV
$\Delta = 2.23$	2.40	2.24	2.14	2.14	eV
$\theta = 90°$	$\theta = 96°$	$\omega = 160°$	$\phi = 20°$	$r = 0.98$	

(55) Dance, J. M.; Mur, J.; Darriet, J.; Hagenmuller, P.; Massa, W.; Kummer, S.; Babel, D. *J. Solid State Chem.* **1986**, *63*, 446.
(56) The magnetism of the single example of unit **3c**,[20] also containing the $Fe_2(OR)_2$ bridge, has not been reported.
(57) Hodgson, D. J. *Prog. Inorg. Chem.* **1975**, *19*, 173.
(58) Hay, P. J.; Thibeault, J. C.; Hoffmann, R. *J. Am. Chem. Soc.* **1975**, *97*, 4884.
(59) Ginsberg, A. P. *Inorg. Chim. Acta Rev.* **1971**, *5*, 45.
(60) Parameters: Tatsumi, K.; Hoffmann, R. *J. Am. Chem. Soc.* **1981**, *103*, 3328. Computational details: Ammeter, J. H.; Bürgi, H.-B.; Thibeault, J. C.; Hoffmann, R. *J. Am. Chem. Soc.* **1978**, *100*, 3686.
(61) Burdett, J. K. *J. Am. Chem. Soc.* **1979**, *101*, 5217.
(62) Shaik, S.; Hoffmann, R.; Fisel, C. R.; Summerville, R. H. *J. Am. Chem. Soc.* **1980**, *102*, 4555.

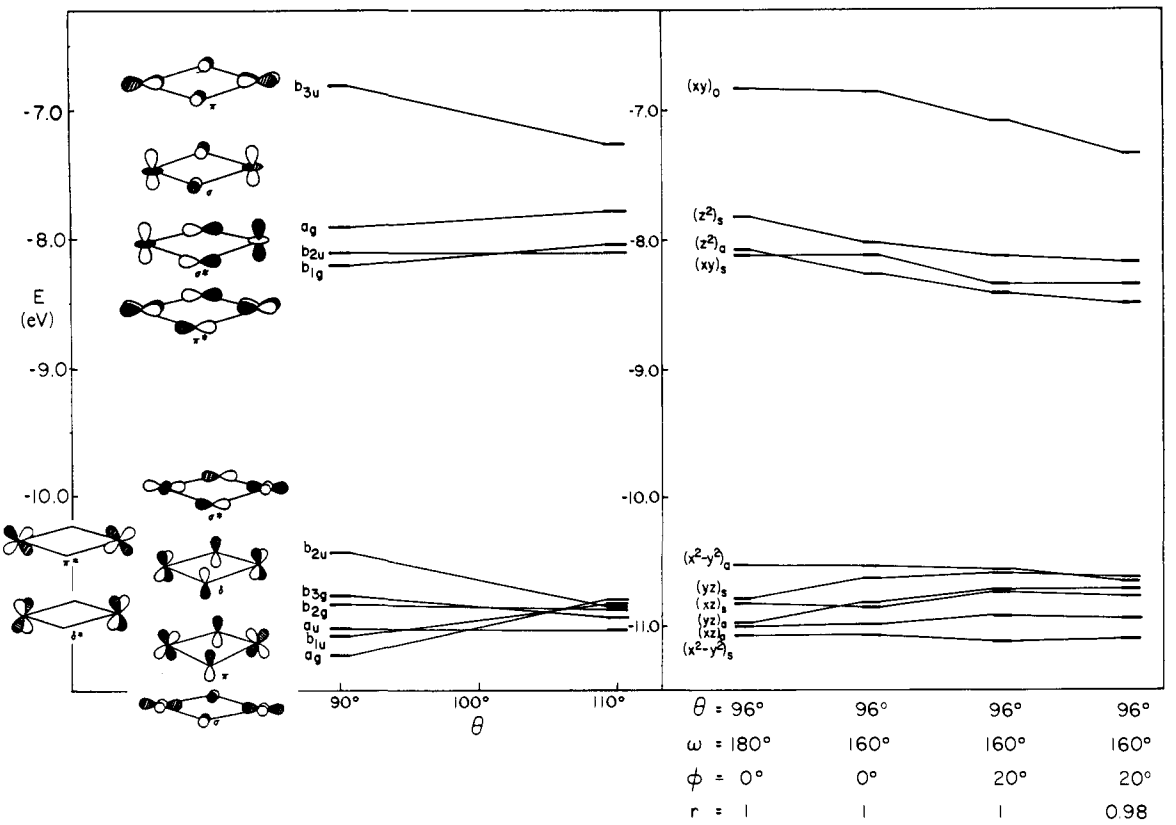

Figure 10. Energies of d-block MOs of $Fe_2(NH_3)_4(OH)_6$. Left: effect of bridge angle θ over the range 90–110° with retention of D_{2h} symmetry; the idealized configuration has θ = 90° and ϵ = 180°. Right: effects of the distortions θ = 96°, ω = 160°, ϕ = 20°, and r = 0.98 applied successively to the idealized configuration.

Again, energy changes can be reduced to overlap considerations. For example, the ω distortion stabilizes $(z^2)_{s,a}$ but destabilizes $(yz)_{s,a}$ because of decreased and increased antibonding interaction, respectively, with the N σ orbitals. Similarly, under the ϕ distortion $(x^2 - y^2)_{s,a}$ and $(xy)_{s,a}$ are stabilized as the terminal ligands are displaced from the xy plane, whereas $(xz)_{s,a}$ and $(yz)_{s,a}$ are destabilized. The r distortion further stabilizes the orbitals in the xy plane. The net effect of the distortions required to attain the observed stereochemistry of $Fe_2(salmp)_2$ is reduction of the values of the two parameters of orbital spacing vs the idealized case. It appears that the distortion of the coordination units results in a stabilization of the e-type orbitals relative to the t_2-type, which is qualitatively consistent with the transition from antiferromagnetic to a ferromagnetic ground state. In contrast to the binuclear Cu(II) case, the bridge angle here appears to have only a contributory role in any possible crossover of magnetic states, rather than a dominant one.

Last, the ferromagnetism of $[Fe_2(salmp)_2]^{0,1-,2-}$, unique to this set of $Fe_2(\mu\text{-}OR)_2$ complexes,[63] has been further confirmed by magnetization,[64] EPR, and Mössbauer spectroscopic measurements.[38] The results of these investigations, which are expected to provide more accurate values of ferromagnetic coupling constants, will be reported subsequently. The complexes examined here are members of an expanding group of newly discovered ferromagnetic compounds. In addition to $[Fe_2(OH)_3(Me_3tacn)_2]^{2+}$ with $S = {}^9/_2$,[23] compounds with $S = {}^9/_2$,[65] 6,[66] 12,[67] and 14[68] and containing Cr or Mn have been discovered. The magnetic character of the complexes $[M_2(salmp)_2]^z$ with these and other metals are of potential significance. In particular, it will be important to learn if the distortions and ferromagnetism encountered here extend to other cases with more than six d electrons.

Acknowledgment. This research was supported by NIH Grant GM 28856. X-ray diffraction equipment was obtained through NIH Grant 1-S10-RR-02247. We thank Dr. R. Mukherjee for preliminary experiments and Professors D. N. Hendrickson and K. Wieghardt for the provision of manuscripts prior to publication.

Supplementary Material Available: Tables of positional and thermal parameters, hydrogen atom positional parameters, interatomic distances and angles, and magnetic susceptibilities for compounds **6**, 7, and **8** (28 pages); listing of calculated and observed structure factors (81 pages). Ordering information is given on any current masthead page.

(63) Several ligated forms of deoxyhemerythrin are ferromagnetic; the bridge structure involving the two Fe(II) centers is unknown but may involve a water molecule: Reem, R. C.; Solomon, E. I. *J. Am. Chem. Soc.* **1987**, *109*, 1216.

(64) Day, E. P., private communication.

(65) Li, Q.; Vincent, J. B.; Libby, E.; Chang, H.-R.; Huffman, J. C.; Boyd, P. D. W.; Christou, G.; Hendrickson, D. N. *Angew. Chem., Int. Ed. Engl.* **1988**, *27*, 1731.

(66) Bino, A.; Johnston, D. C.; Goshorn, D. P.; Halbert, T. R.; Stiefel, E. I. *Science* **1988**, *241*, 1479.

(67) Caneschi, A.; Gatteschi, D.; Laugier, J.; Rey, P.; Sessoli, R.; Zanchini, C. *J. Am. Chem. Soc.* **1988**, *110*, 2795.

(68) Boyd, P. D. W.; Li, Q.; Vincent, J. B.; Folting, K.; Chang, H.-R.; Streib, W. E.; Huffman, J. C.; Christou, G.; Hendrickson, D. N. *J. Am. Chem. Soc.* **1988**, *110*, 8537.